

## TESTING GAUSSIAN RANDOM HYPOTHESIS OF THE COSMIC MICROWAVE BACKGROUND TEMPERATURE ANISOTROPIES IN THE 3-YEAR WMAP DATA

LUNG-YIH CHIANG<sup>1</sup> PAVEL D. NASELSKY<sup>1</sup> PETER COLES<sup>2</sup>  
chiang@nbi.dk, naselsky@nbi.dk, peter.coles@nottingham.ac.uk*Subject headings:* cosmology: cosmic microwave background — cosmology: observations — methods: data analysis*Submitted to the Astrophysical Journal Letter*

## ABSTRACT

We test in the 3-year WMAP data for the Gaussian random hypothesis on the de-biased internal linear combination (DILC) map. We test the phases for  $\ell \leq 10$  for their uniformity, randomness, and correlation with those of the foreground templates. These phases are uniformly distributed but those  $\ell \leq 5$  are skewed and phase differences avoid 0 or  $\pi$ . For  $\ell = 3$  and 6 modes the phases cross correlate with the foregrounds, indicating contamination. We also use 1-dimensional Fourier representation to assemble  $a_{\ell m}$  into the  $\Delta T_{\ell}(\varphi)$  for each  $\ell$  and test the extrema statistics, assuming that the maximum and minimum peaks should be randomly distributed. The significance level is less than 0.5% and peaks are concentrated around the origin  $\varphi = 0$ . Since phases are defined in Galactic coordinates, the results strongly suggest that the 9 harmonics are contaminated with the foregrounds.

## 1. INTRODUCTION

Since the release of the 1-year Wilkinson Microwave Anisotropy Probe (WMAP) data (Bennett et al. 2003b,c; Spergel et al. 2003; Hinshaw et al. 2003b; Komatsu et al. 2003), great efforts have been made for the search and detection of non-Gaussianity of the cosmic microwave background (CMB) temperature fluctuations via various approaches and methods (Chiang et al. 2003; Coles et al. 2004; Park 2004; Eriksen et al. 2004c; Vielva et al. 2004; Copi, Huterer & Starkman 2004; Cabella et al. 2004; Hansen et al. 2004; Mukherjee & Wang 2004; Larson & Wandelt 2004; Dineen & Coles 2006).

With 3 years data and the improvement on foreground cleaning, the WMAP team have produced the de-biased internal linear combination (DILC) map, which is suitable for analysis over the full sky up to  $\ell \leq 10$  (Spergel et al. 2006; Hinshaw et al. 2006). The statistics of these low multipole modes provide valuable information with cosmological significance, particularly about statistical isotropy of the CMB.

The 3-year data analyzed by the WMAP team is claimed to be Gaussian. Non-Gaussianity, if detected, could result from primordial origin (Bartolo et al. 2004), possible foreground residues from cleaning (Naselsky, Doroshkevich & Verkhodanov 2003, 2004; Dineen & Coles 2003; Naselsky & Novikov 2005) and correlated noise, therefore one has to be cautious on non-Gaussianity detected to be attributed to primordial origin. The concept of internal linear combination to obtain reasonable CMB signal is via tuning the weighting coefficients to minimize the variance of the foregrounds. One should note that the variance is only minimized but not zero. Since phases faithfully reflect morphology (Chiang 2001), comparison between the phases of the DILC and the derived foregrounds shall give some indications on foreground contaminations and statistical isotropy manifest itself in the

phase information. Although it is this connection with morphology that phases are rotationally invariant, some of the issues such as north-south asymmetry (Eriksen et al. 2004b) and the alignment of multipole vectors (Schwarz et al. 2004; Land & Magueijo 2005) are measured in a preferred coordinates, i.e. Galactic coordinates, where the phases are defined, detection of non-uniform or non-random phases therefore shed light on those peculiarities.

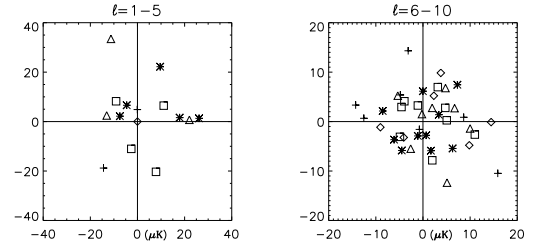


FIG. 1.— The  $a_{\ell m}$  for  $\ell \leq 10$  are plotted on the Argand plane. The amplitudes are in unit of  $\mu\text{K}$  and only  $m > 0$  modes are displayed. The signs  $\diamond$ ,  $+$ ,  $\triangle$ ,  $\square$  and  $*$  represent  $\ell = 1 - 5$  on the left,  $\ell = 6 - 10$  on the right panel, respectively. Note that 12 out of 15 phases of  $\ell \leq 5$  are in the first 2 quadrants, among which 6 are near 0 or  $\pi$ .

## 2. GAUSSIAN RANDOM HYPOTHESIS OF THE CMB

The statistical characterization of CMB anisotropies on a sphere can be expressed as a sum over spherical harmonics:

$$\Delta T(\theta, \varphi) = \sum_{\ell=0}^{\infty} \sum_{m=-\ell}^{\ell} a_{\ell m} Y_{\ell m}(\theta, \varphi), \quad (1)$$

where the  $Y_{\ell m}(\theta, \varphi)$  are spherical harmonic functions defined in terms of the Legendre polynomials  $P_{\ell m}$  using

$$Y_{\ell m}(\theta, \varphi) = (-1)^m \sqrt{\frac{(2\ell+1)(\ell-m)!}{4\pi(\ell+m)!}} P_{\ell m}(\cos \theta) \exp(im\varphi) \quad (2)$$

<sup>1</sup> Niels Bohr Institute, Blegdamsvej 17, DK-2100 Copenhagen, Denmark<sup>2</sup> School of Physics & Astronomy, University of Nottingham, University Park, Nottingham NG7 2RD, United Kingdom

and the  $a_{\ell m}$  are complex coefficients which can be expressed with  $a_{\ell m} = |a_{\ell m}| \exp(i\phi_{\ell m})$ . In standard cosmological models (i.e. those involving the simplest forms of inflation) these fluctuations constitute a realization of a statistically homogeneous and isotropic Gaussian stochastic process, or random field, defined over the celestial sphere (Bardeen et al. 1986; Bond & Efstathiou 1987). The formal definition of such a Gaussian random field requires that the real and imaginary parts of the  $a_{\ell m}$  are independent and identically distributed according to a Gaussian probability density, so that the moduli  $|a_{\ell m}|$  have a Rayleigh distribution and the phases  $\phi_{\ell m}$  are uniformly random on the interval  $[0, 2\pi]$ . The Central Limit Theorem guarantees that the superposition of a large number of harmonic modes will tend to a Gaussian as long as the phases are random, and this furnishes a weaker definition of Gaussianity. Moreover, statistical isotropy manifest itself in phase properties. Because of the importance of phases in both these definitions, we focus on their measured properties as probes of departures from Gaussianity. Methods to test the random phase hypothesis (RPH) are proposed by Chiang, Coles & Naselsky (2002); Chiang, Naselsky & Coles (2004); Dineen, Rocha and Coles (2005); Naselsky et al. (2004); Chiang & Naselsky (2006).

In this Letter we test the phase properties of the 3-year DILC map recently produced by the WMAP. Due to the resemblance between 1-year ILC and 3-year DILC maps, in the following analysis we compare both maps.

In Fig.1 we show plot on the Argand plane the  $a_{\ell m}$  of the DILC map for  $\ell \leq 10$  (amplitudes  $|a_{\ell m}|$  in unit of  $\mu\text{K}$ .). Due to the conjugate properties of the  $a_{\ell m}$  for real singal, we plot only  $a_{\ell m}$  modes of  $m \geq 1$  and omit all  $m = 0$  modes. Note the non-uniformity of the phases for  $\ell \leq 5$ .

### 3. TESTING ON RANDOM PHASE HYPOTHESIS

We use Kuiper's statistic (Kuiper 1960) (KS) to test on the random phase hypothesis. The KS can be viewed as a variant of Kolmogorov–Smirnov test designed to cope with circular data. The standard Kolmogorov–Smirnov statistic is taken as the maximum distance of the cumulative probability distribution against the theoretical one:  $D = \max_{-\infty < x < \infty} |S_N(x) - P(x)|$ . For a circular function, however, one needs to take into account the maximum distance both above and below the theoretical probability  $P(x)$ :

$$V = D_+ + D_- = \max_{-\infty < x < \infty} [S_N(x) - P(x)] + \max_{-\infty < x < \infty} [P(x) - S_N(x)]$$

The significance level  $\alpha$  in accord with the null hypothesis can be calculated from  $\alpha = Q_{\text{Kuiper}}(V[\sqrt{N} + 0.155 + 0.24/\sqrt{N}])$  and  $Q_{\text{Kuiper}}(\lambda) = 2 \sum_{j=1}^{\infty} (4j^2 \lambda^2 - 1) e^{-2j^2 \lambda^2}$ ,  $N$  is the number of data points.

	$\phi_{\ell m}$ of $\ell \leq 5$	$\phi_{\ell m}$ of $6 \leq \ell \leq 10$	all $\phi_{\ell m}$ of $\ell \leq 10$
ILC	38.74%	90.91%	73.55%
DILC	30.63%	98.09%	66.14%

TABLE 1

THE SIGNIFICANCE LEVEL  $\alpha$  IN ACCORD WITH THE UNIFORM DISTRIBUTION HYPOTHESIS OF THE PHASES OF THE 1-YEAR ILC AND 3-YEAR DILC MAPS.

In the following 3 tests on the *uniformity* of phases, on the *randomness* of phases by taking difference of

phases with fixed separation  $(\Delta\ell, \Delta m)$ , and on the cross-correlation of each  $\ell$  between DILC and the foregrounds by  $\Delta\phi_{\ell m}^X = \phi_{\ell m}^{\text{dilc}} - \phi_{\ell m}^{\text{FG}}$ , the null hypothesis is uniformity between 0 and  $2\pi$ . The reason is that the difference of 2 random phase sequences should still be uniformly random (one random phase sequence is enough for a  $\Delta\phi$  sequence to be random).

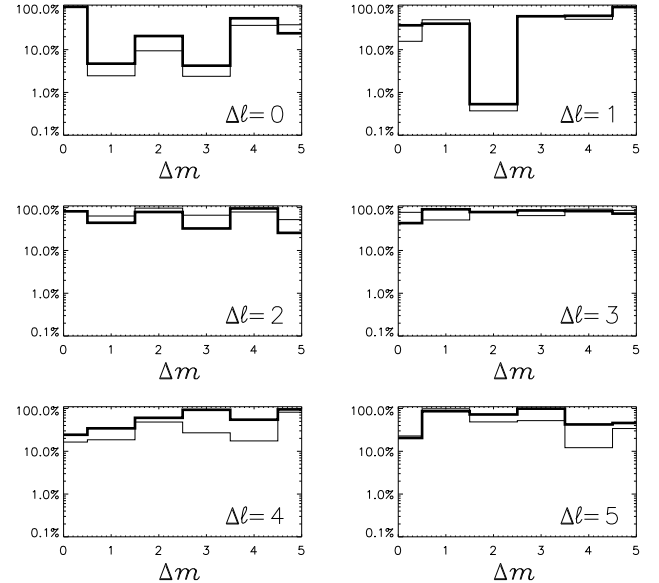


FIG. 2.— Significance levels of randomness with separation  $(\Delta\ell, \Delta m)$ . The thick and thin lines are from 3-year DILC and 1-year ILC maps, respectively.

We firstly test the uniformity of the phases for  $1 \leq \ell \leq 5$ ,  $6 \leq \ell \leq 10$  and all phases for  $\ell \leq 10$ . The phases of  $m = 0$  modes are excluded in our test. Table 1 shows that for the 3-year DILC, while the phases are uniformly distributed with significance  $\alpha \sim 98\%$  for  $6 \leq \ell \leq 10$ , for  $\ell \leq 5$  it is merely 31%, which can be easily seen in Fig.1 that the phases are in the first 2 quadrants, and they are less uniformly distributed than the 1-year ILC map. Overall, the phases of the 3-year DILC map for  $\ell \leq 10$  are reasonably uniformly distributed with significance 66%.

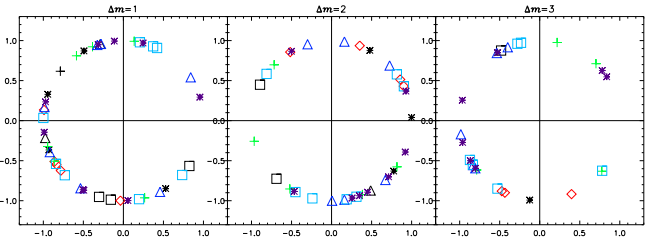


FIG. 3.— Phase difference for  $\Delta m = 1, 2$  and 3 for all  $\phi_{\ell m}^{\text{dilc}}$ ,  $1 \leq \ell \leq 10$ ,  $1 \leq m \leq \ell$  plotted on a unit circle. The significance levels of uniformity are 4.70%, 20.85% and 4.21%, respectively. The signs  $\diamond$ ,  $+$ ,  $\Delta$ ,  $\square$  and  $*$  in black represent phase difference within  $\ell = 1 - 5$ , respectively, and in color within  $\ell = 6 - 10$ , respectively.

Randomness of phases is tested by the all  $\Delta\phi^{\text{dilc}}(\Delta\ell, \Delta m) = \phi_{\ell+\Delta\ell, m+\Delta m}^{\text{dilc}} - \phi_{\ell m}^{\text{dilc}}$ . In Fig.2 we show the significance levels for randomness between phases. There are 3 separations with significantly low  $\alpha = 4.70\%$ , 4.21% and 0.53% for  $(\Delta\ell, \Delta m) = (0, 1)$ ,  $(0, 3)$  and  $(1, 2)$ , respectively, indicating that the phases are strongly coupled. It is complicated to understand coupling across both  $\ell$  and  $m$  for  $(\Delta\ell, \Delta m) = (1, 2)$ . Nevertheless, as the first

2 are coupling between azimuthal number  $m$  within each  $\ell$ , with which the composite maps are drawn, we plot in Fig.3 the sequences of phase difference  $\Delta\phi^{\text{dilc}}(0,1)$  and  $\Delta\phi^{\text{dilc}}(0,3)$  on a unit circle (or  $\exp(i\Delta\phi^{\text{dilc}}(1,0))$  on an Argand plane). For both distributions one can see the voids around  $\Delta\phi = 0$  which cause the significance levels below 5%. We also include (0,2) in Fig.3 for comparison, which has the tendency of phase differences to avoid  $\pi$ .

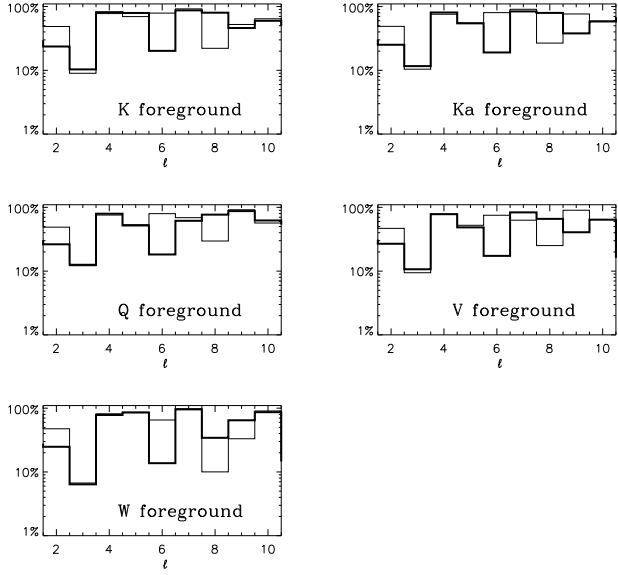


FIG. 4.— Significance levels on the cross-correlation of phases at each  $\ell$  between the DILC (thick lines) and the WMAP foreground maps at K, Ka, Q, V and W channels, respectively. For comparison, the thin lines are those between 1-year ILC and 1-year foreground maps.

#### 4. CROSS-CORRELATION BETWEEN DILC AND THE FOREGROUND MAPS

Since the DILC map is obtained from internal combination of the frequency maps, some foreground residues might be left in the resultant map. Based on the assumption that CMB signal should not correlate with the foregrounds, and that the characteristic of phases reflect the morphology of the CMB anisotropy pattern, we also test the cross-correlation of phases for DILC and WMAP 3-year foreground maps at K, Ka, Q, V and W channels. The foreground maps we test are the sum of the synchrotron, free-free and dust templates. We take the phase difference  $\Delta\phi_{\ell m}^X = \phi_{\ell m}^{\text{dilc}} - \phi_{\ell m}^{\text{FG}}$  for each  $\ell$ , assuming such  $\Delta\phi_{\ell m}$  at each  $\ell$  should be uniformly distributed. In Fig.4 one can see that for  $\ell = 3$  and 6 the UILC phases have correlation with the foregrounds with significance around 10%. One particular point about quadrupole is, easily seen from Fig.1, 2 of the 3 quadrupole phases are near 0 and  $\pi$ , and for  $\ell = 6$ , in Fig.3 (shown in red diamond sign), the phase difference for  $\Delta m = 1$  are clustered.

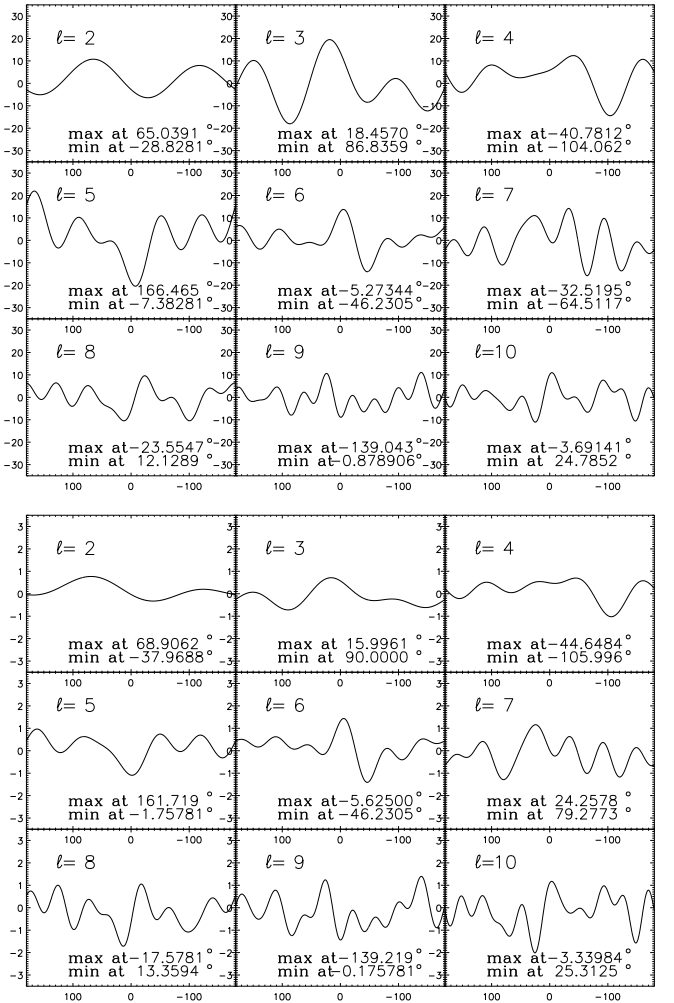


FIG. 5.— The  $\Delta T_\ell(\varphi)$  distribution for each  $\ell$  from the DILC map by assembling  $\sum_m a_{\ell m}^{\text{dilc}} \exp(im\varphi)$  (top panel, in which the unit of  $y$  axis is  $\mu\text{K}$ ) and by assembling only the phase part :  $\sum_m \exp(i\phi_{\ell m}^{\text{dilc}}) \exp(im\varphi)$  (bottom). In order to match the convention of Galactic longitude coordinate (for comparison with, e.g. Fig.14 in Hinshaw et al. (2006)), the  $\varphi$  axis is plotted reversely. In each figure we indicate the locations of the extrema.

#### 5. EXTREMA STATISTICS

The  $\Delta m$  phase coupling in each  $\ell$  lead to the signal departing from Gaussianity. Following Chiang & Naselsky (2006) we present the phase coupling effect by assembling the  $a_{\ell m}$  (now only single variable  $m$ ) with inverse Fourier transform:

$$\Delta T_\ell(\varphi) = \sum_m a_{\ell m}^{\text{dilc}} \exp(im\varphi), \quad (4)$$

where in the summation for the negative  $m$  we use conjugate  $a_{\ell m}$  to make  $\Delta T_\ell$  real. The morphology of the signal is similar to the signal  $\Delta T(\theta, \varphi)$  for each  $\ell$  by summing over all  $\theta$  onto  $\varphi$  direction. Although such presentation loses information on one dimension, regardless of the  $a_{\ell m}$  being spherical harmonic coefficients, the statistics registered in the 1D complex  $a_{\ell m}$  should still manifest themselves in the 1D  $\Delta T$  curves. In Fig.5 we plot  $\Delta T(\varphi)$  summing from the DILC  $a_{\ell m}$  (top), and from the whitened DILC :  $a_{\ell m}/|a_{\ell m}|$  (bottom). If the signal is Gaussian, the locations of the highest and lowest peaks should randomly distributed in

$\varphi$  between  $-180^\circ$  and  $180^\circ$ . We plot in Fig.6 the distribution of these extrema locations in a unit circle.

In Table 2 we list the significance of the distribution of the extrema locations. Not only do they show , the peak locations cluster in  $\varphi = 0$ . In Fig.4 the  $\ell = 3$  and 6 show significant cross correlation with the foregrounds, we then test the peak distribution by excluding the 4 extrema of these 2 modes. Although the statistics are slightly better, they are still below 5%.

	3-y DILC	Whitened 3-y DILC
all peaks $\ell \leq 10$	0.450%	0.552 %
excluding peaks of $\ell = 3, 6$	2.759%	4.218 %

TABLE 2

SIGNIFICANCE OF THE DISTRIBUTION OF THE EXTREMA LOCATIONS IN  $T_\ell$ .

## 6. CONCLUSION

In this letter we test the Gaussian random hypothesis of the CMB temperature anisotropies. Due to the resemblance of the 1-year ILC and 3-year DILC maps, all the peculiarities still exist, as mentioned in Spergel et al. (2006). We find that the phase differences avoid 0 in each  $\ell$ . The phases of  $\ell = 3$  and 6 are correlated with those of the foregrounds. We also test the extrema statistics using Fourier representation for each  $\ell$ . The peaks are concen-

trated around the origin of the Galactic coordinates where phases are defined. With the extrema statistics, one can conclude that the 9 multipoles are statistically anisotropic with significance less than 5% and the sources are the foregrounds.

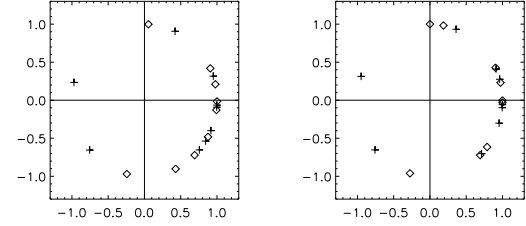


FIG. 6.— The distribution of the extrema locations of  $\Delta T_\ell(\varphi)$  as shown in Fig.5. The angle of the unit circle denotes the location  $\varphi$ . The left panel is for the DILC  $\Delta T_\ell(\varphi)$ , and the right for the whitened DILC  $\Delta T_\ell(\varphi)$ . The  $\diamond$  sign denotes maxima and the  $+$  sign minima.

## ACKNOWLEDGMENTS

We acknowledge the use of the NASA Legacy Archive for extracting the *WMAP* data. We also acknowledge the use of HEALPIX<sup>3</sup> package (Górski, Hivon & Wandelt 1999) to produce  $a_{\ell m}$  from the *WMAP* data and the use of GLESP<sup>4</sup> package (Doroshkevich et al. 2003).

## REFERENCES

Banday, A. J., Zaroubi, S., Gorski, K. M., 2000, ApJ, 533, 575  
 Bardeen, J. M., Bond, J. R., Kaiser, N., Szalay, A. S., 1986, ApJ, 304, 15  
 Bartolo, N., Komatsu, E., Matarrese, S., Riotto, A., 2004, Phys. Rep., 402, 103  
 Bennett, C. L., et al., 2003, ApJS, 148, 1  
 Bennett, C. L., et al., 2003, ApJS, 148, 97  
 Bond, J. R., Efstathiou, G., 1987, MNRAS, 226, 655  
 Cabella, P., Hansen, F., Marinucci, D., Pagano, D., Vittorio, N., 2004, Phys. Rev. D, 69, 063007  
 Chiang, L.-Y., 2001, MNRAS, 325, 405  
 Chiang, L.-Y., Coles, P., 2000, MNRAS, 311, 809  
 Chiang, L.-Y., Coles, P., Naselsky, P. D., 2002, MNRAS, 337, 488  
 Chiang, L.-Y., Naselsky, P. D., Coles, P., 2004, ApJL, 602, 1  
 Chiang, L.-Y., Naselsky, P. D., Verkhodanov, O. V., Way, M. J., 2003, ApJ, 590, L65  
 Chiang, L.-Y., Naselsky, P. D., 2006, Int. J. Mod. Phys. D in press (astro-ph/0407359)  
 Coles, P., Barrow, J. D., 1987, MNRAS, 228, 407  
 Coles, P., Chiang, L.-Y., 2000, Nature, 406, 376  
 Coles, P., Dineen, P., Earl, J., Wright, D., 2004, MNRAS, 350, 989  
 Copi, C. J., Huterer, D., Starkman, G. D., 2004, Phys. Rev. D, 70, 043515  
 Dineen, P., Coles, P., 2003, MNRAS, 347, 52  
 Dineen, P., Coles, P., 2006, MNRAS submitted (astro-ph/0511802)  
 Dineen, P., Rochar, G., Coles, P., 2005, MNRAS, 358, 1285  
 Doroshkevich, A. G., Naselsky, P. D., Verkhodanov, O. V., Novikov, D. I., Turchaninov, V. I., Novikov, I. D., Christensen, P. R., Chiang, L.-Y., 2003, Int. J. Mod. Phys. D, 14, 275  
 Eriksen, H. K., Hansen, F. K., Banday, A. J., Gorski, K. M., Lilje, P. B., 2004, ApJ, 605, 14  
 Eriksen, H. K., Novikov, I. D., Lilje, P. B., Banday, A. J., Gorski, K. M., 2004, ApJ, 612, 64  
 Ferreira, P., Magueijo, J., Gorski, K. M., 1998, ApJ, 503, L1  
 Gaztanaga, E., Wagg, J., 2003, Phys. Rev. D, 68, 021302  
 Górski, K. M., Hivon, E., Wandelt, B. D., 1999, in A. J. Banday, R. S. Sheth and L. Da Costa, Proceedings of the MPA/ESO Cosmology Conference “Evolution of Large-Scale Structure”, PrintPartners Ipskamp, NL  
 Hansen, F. K., Cabella, P., Marinucci, D., Vittorio, N., 2004, ApJL, 607, 67  
 Hinshaw, G., et al., 2003, ApJS, 148, 135  
 Hinshaw, G., et al., 2006, ApJ submitted (astro-ph/0603451)  
 Komatsu, E., et al., 2003, ApJS, 148, 119  
 Kuiper, N. H., 1960, Proceedings of the Koninklijke Nederlandse Akademie van Wetenschappen, Series A, Vol 63  
 Land, K., Jagueijo, J., 2005, Phys. Rev. Lett., 95, 071301  
 Larson, D. L., Wandelt, B. D., 2004, ApJL, 613, 85  
 Matsubara, T., 2003, ApJL, 591, 79  
 Mukherjee, P., Wang, Y., 2004, ApJ, 613, 51  
 Naselsky, P. D., Chiang, L.-Y., Verkhodanov, O. V., Novikov, I. D., 2005, Int. J. Mod. Phys. D, 14, 1273  
 Naselsky, P. D., Chiang, L.-Y., Olesen, P., Novikov, I. D., 2005, Phys. Rev. D, 72, 3512  
 Naselsky, P. D., Doroshkevich, A., Verkhodanov, O. V., 2003, ApJL, 599, 53  
 Naselsky, P. D., Doroshkevich, A., Verkhodanov, O. V., 2004, MNRAS, 349, 695  
 Naselsky, P. D., Novikov, I. D., 2005, Int. J. Mod. Phys. D, 10, 1769  
 Park, C.-G., 2004, MNRAS, 349, 313  
 Schwarz, D. J., Starkman, G. D., Huterer, D., Copi, C. J., 2004, Phys. Rev. Lett., 93, 221301  
 Spergel, D. N., et al., 2006, ApJ submitted (astro-ph/0603449)  
 Spergel, D. N., et al., 2003, ApJS, 148, 175  
 Tegmark, M., de Oliveira-Costa, Á., Hamilton, A., 2003, Phys. Rev. D, 68, 123523  
 Vielva, P., Martínez-González, E., Barreiro, R. B., Sanz, J. L., Cayon, L., 2004, ApJ, 609, 22  
 Watts, P. I. R., Coles, P., Melott, A., 2003, ApJL, 589, 61

<sup>3</sup> <http://www.eso.org/science/healpix/><sup>4</sup> <http://www.glesp.nbi.dk>